The Leachability of Calcium Aluminate Phases in Slags for the Extraction of Alumina

Fabian Imanasa Azof[1], Leiv Kolbeinsen[2] and Jafar Safarian[3]
1. PhD student
2. Professor
3. Associate Professor
Norwegian University of Science and Technology (NTNU), Department of Materials
Science and Engineering, Trondheim, Norway
Corresponding author: fabian.i.azof@ntnu.no

Abstract

Alumina is used primarily as feedstock for aluminum production. It occurs naturally in bauxite and clay and other minerals, and can be concentrated in industrial by-products such as coal gangue, fly ash, blast furnace slag, etc. The hydrometallurgical treatment of bauxite to recover alumina has been widely adopted industrially since the Bayer process was first employed commercially. However, the sustainability of alumina production by this means is less than ideal, due to the high production rate of poorly utilized and highly alkaline by-product that the process yields; bauxite residue or red mud. On the other hand, digestion of alumina-containing slags produced by reduction of bauxite results in no red mud production. In this work, the leachability of binary phases of CaO and Al_2O_3 in slags is studied under given conditions of temperature and time. Advanced characterization techniques are used to study the chemical composition, phases and microstructure of the slags and the digestion products. It is apparent that the leachability of a phase affects that of other phases. A less leachable phase could hinder the leachability of a more leachable phase. The experimental data shows that the leaching rate of slag from highest to the lowest is $CaO.Al_2O_3$, $3CaO.Al_2O_3$, and $CaO.2Al_2O_3$, respectively.

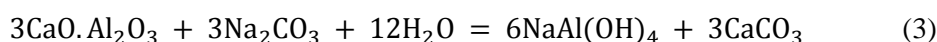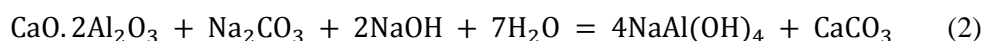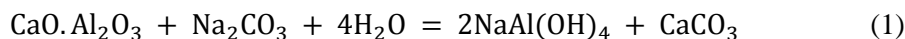**Keywords:** Alumina, calcium oxide, slag, smelting reduction, leachability.

1. Introduction

Alumina (Al_2O_3) is found in different sources in nature, i.e. bauxite, nepheline, clay, and industrial by products such as coal gangue, fly ash, blast furnace slag, etc. However, metallurgical alumina produced from bauxite still dominates the world's alumina production due to the technical and economic feasibility of the Bayer process. A high-grade bauxite, with a mass ratio of Al_2O_3 to SiO_2 greater than 6.25 [1, 2], and/or high Al_2O_3 to Fe_2O_3 ratio [3], can be directly treated without much disruption along the sequential treatment steps of the Bayer process. However, regions that are far from the equatorial zone, who have more karst bauxite than lateritic deposits, generally need more rigorous (and costly) leaching conditions, or use a pyro-hydrometallurgical process to treat the bauxite. This is because in general, the mineralogical composition of laterite is $Al(OH)_3$ (gibbsite) and $AlO(OH)$ (boehmite), while karst bauxite is $AlO(OH)$ (boehmite) and $AlO(OH)$ (diaspore), the latter being significantly more difficult to process [1].

An alternative method to beneficiate bauxite ore with high iron content is by smelting reduction as our recent studies in *research domain 5-Materials and Society* in SFI-metal production shows its feasibility in avoiding red mud production [4, 5]. It produces pig iron as a by-product, and a calcium aluminate slag as the source of alumina. This approach is the traditional Pedersen process [6]. Although there is no commercial production of alumina by this process, there has been research on hydrometallurgical treatment of calcium-aluminate slags. Lundquist and Leitch [7], Tong and Li [8], and Wang et al. [9] investigated the leachability of three calcium

aluminates ($12CaO.7Al_2O_3, 3CaO.Al_2O_3, 4CaO.Al_2O_3.Fe_2O_3$). These were produced from the lime-soda sinter process in a different solvent, calcium aluminate produced by smelting reduction of red mud with the addition of TiO_2, and MgO-containing calcium aluminate phases ($12CaO.7Al_2O_3$ and $\gamma - 2CaO.SiO_2$), and from blast furnace slag with the addition of Na_2O, respectively. Other researchers showed the synergistic effect of $12CaO.7Al_2O_3$ and $CaO.Al_2O_3$ on alumina leachability [10].

However, the leaching behavior of each calcium aluminate phase in the binary system is not yet clear. The leaching reaction of three calcium aluminate phases in alumina production are described below in Equations (1 – 3).

$$CaO.Al_2O_3 + Na_2CO_3 + 4H_2O = 2NaAl(OH)_4 + CaCO_3 \qquad (1)$$

$$CaO.2Al_2O_3 + Na_2CO_3 + 2NaOH + 7H_2O = 4NaAl(OH)_4 + CaCO_3 \qquad (2)$$

$$3CaO.Al_2O_3 + 3Na_2CO_3 + 12H_2O = 6NaAl(OH)_4 + 3CaCO_3 \qquad (3)$$

To gain proper understanding about these slags' digestion, the leachability of CaO- and Al_2O_3-containing phases in the calcium aluminate slags produced from high purity oxides at elevated temperature is studied in this present work.

2. Experimental Procedure

The experimental procedure consisted mainly of materials preparation and characterization, leaching set up and results analysis. A procedural flow chart is presented in Figure 1.
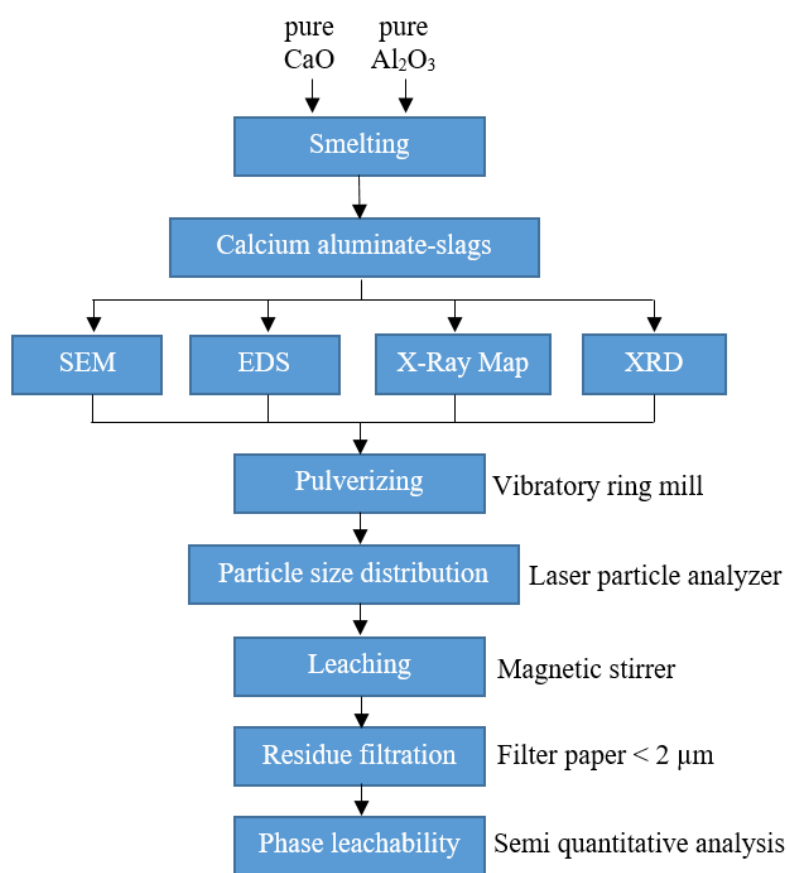

Figure 1. Flow chart of the experimental procedure.

2.1.   Materials Preparation and Characterization

Two synthetic slags of CaO–Al$_2$O$_3$ system, named here Slag I and Slag II, were prepared by smelting the proportioned mixture of high purity CaO (96 wt.%) and Al$_2$O$_3$ (99.9 wt.%) powders inside graphite crucibles at 1650 ^{o}C for 1 hour by means of 75 kVA induction furnace. As can be seen in Figure 2, the target compositions of slag I and II were 33 wt.% CaO – 67 wt.% Al$_2$O$_3$ and 38 wt.% CaO – 62 wt.% Al$_2$O$_3$, respectively. The heating rate was kept slow at 15 ^{o}C/min up to 1000 ^{o}C to remove hydrates and moisture in the mixture, then 30 ^{o}C/min until reaching the targeted smelting temperature. The crucible was air cooled inside the furnace at 28 ^{o}C/min from 1650 ^{o}C to 1300 ^{o}C, and the rate decreased exponentially until it reached room temperature. A Tungsten/Rhenium alloy thermocouple with alumina insulating tube and wired with molybdenum alloy was inserted in a graphite thermo-well and fixed to the wall of the graphite crucible to measure the temperature inside of the crucible.

The crucible was crushed and the slags were collected and ground with a vibratory ring mill at 800 rpm for one minute. The size distribution was measured by laser particle analyzer, which gives 10 μm and 14 μm as the D_{50} value for slag I and II, respectively.
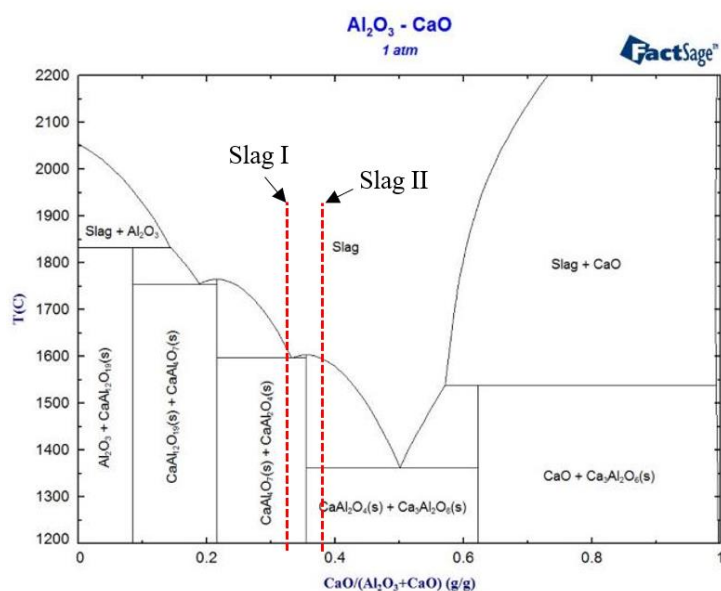

Figure 2. Target composition of slag I and slag II in CaO–Al$_2$O$_3$ phase diagram from FactSage database.

2.2.   Leaching of Slags

The leaching experiments were done in a 50 mL glass beaker with a magnetic stirrer for agitation. The speed for the magnetic stirrer was 400 rpm. The glass beaker was partially submerged inside a water bath that was heated on top of a hot plate to minimise solution temperature variation. The solvent concentration was fixed at 120 g/L Na$_2$CO$_3$ and 7 g/L NaOH based on the literature [8, 9, 11]. To compensate for evaporation during leaching and ensure the proper reactions occurs, the amount of Na$_2$CO$_3$ used is 4 times the stoichiometry. The liquid to solid ratio is 20 and leaching temperature was 45 ^{o}C, 60 ^{o}C, and 75 ^{o}C with 30 minutes of holding time. The slag powder sample was added to the solvent after it reached the target temperature. After the leaching, all of the solution and remaining residue in the beaker was filtered using an ashless grade of quantitative filter paper with fine pores (< 2 μm). The residue

was washed with distilled water several times to ensure there is no alkali left, to avoid further reaction with the slag. It was then dried at 100 $^{\circ}$C in an oven overnight, before being weighed and chemically analyzed by XRD with 5 – 75 degree diffraction angle and 0.01 degree step size.

3.   Results and Discussion

3.1.   Characteristics of Slags

The chemical and phase composition of slags as calculated by FactSage, Backscattered Electron (BSE) imaging, X-Ray elements map, and X-Ray Diffraction (XRD) are shown consecutively in Table 1, Figures 3 – 5.

It can be seen in Figure 3, which is confirmed by XRD results in Figure 5, that Slag I has $CaO.Al_2O_3$ (abbreviated as CA) and $CaO.2Al_2O_3$ (abbreviated as CA_2), while Slag II has CA and $3CaO.Al_2O_3$ (abbreviated as C_3A). This result agrees with the binary system of $CaO–Al_2O_3$ in literature [12, 13]. There is no $12CaO.7Al_2O_3$ observed in Slag II, as it is an unstable phase in anhydrous $CaO–Al_2O_3$ system as reported by Nurse et al. [14].

Table 1. Chemical composition of synthetic slags.

Sample name	CaO (wt.%)	Al_2O_3 (wt.%)	CA phase (wt.%)	CA_2 phase (wt.%)	C_3A phase (wt.%)
Slag I	33	67	84	16	-
Slag II	38	62	91	-	9

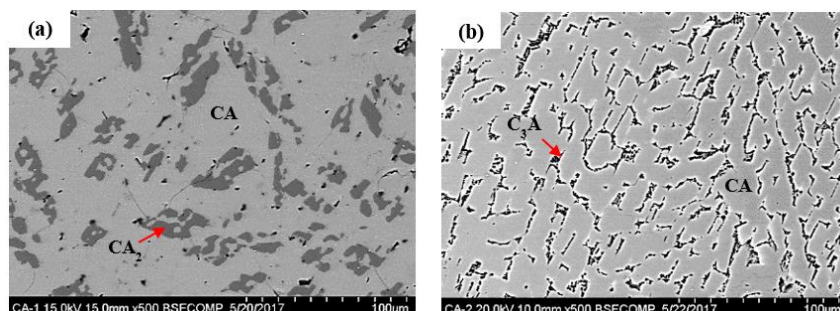**Figure 3. Backscattered electron image of two synthetic slags. (a) Slag I consists of $CaO.Al_2O_3$ (CA) and $CaO.2Al_2O_3$ (CA_2) phases. (b) Slag II consists of $CaO.Al_2O_3$ (CA) and $3CaO.Al_2O_3$ (C_3A) phases.**
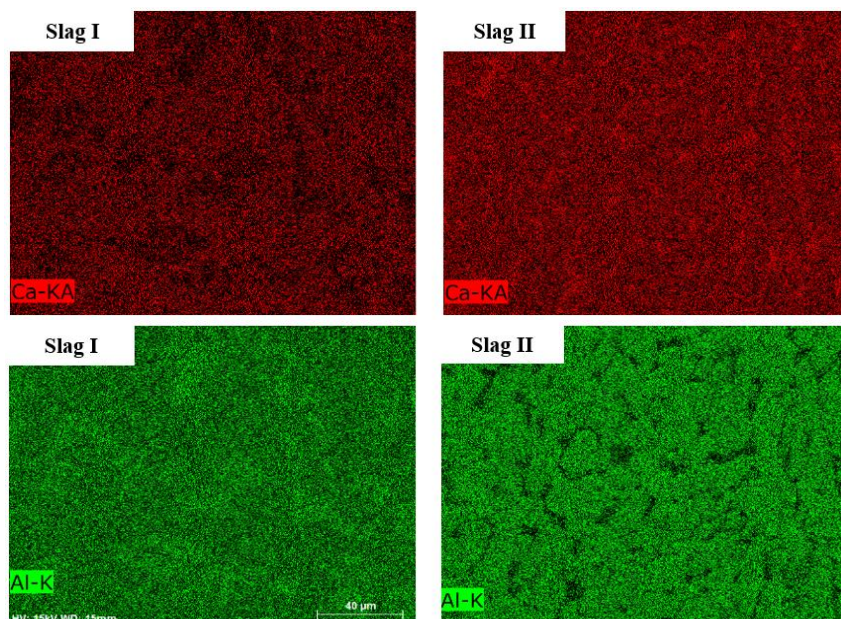
Figure 4. X-Ray element mapping of Slag I and II.

As shown in Figure 4, X-Ray element mapping of Slag I indicates that the matrix has both Calcium and Aluminum, and the secondary phase is rich in Aluminum. On the other hand, in Slag II the secondary phase is richer in Calcium than Aluminum.
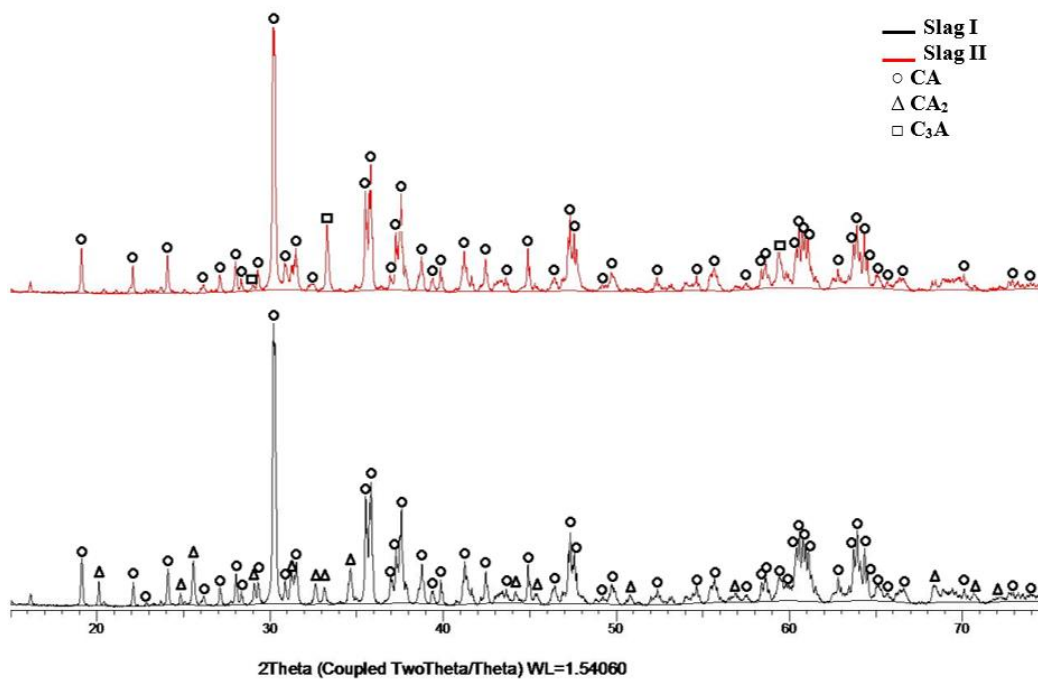

Figure 5. XRD pattern of Slag I and II.
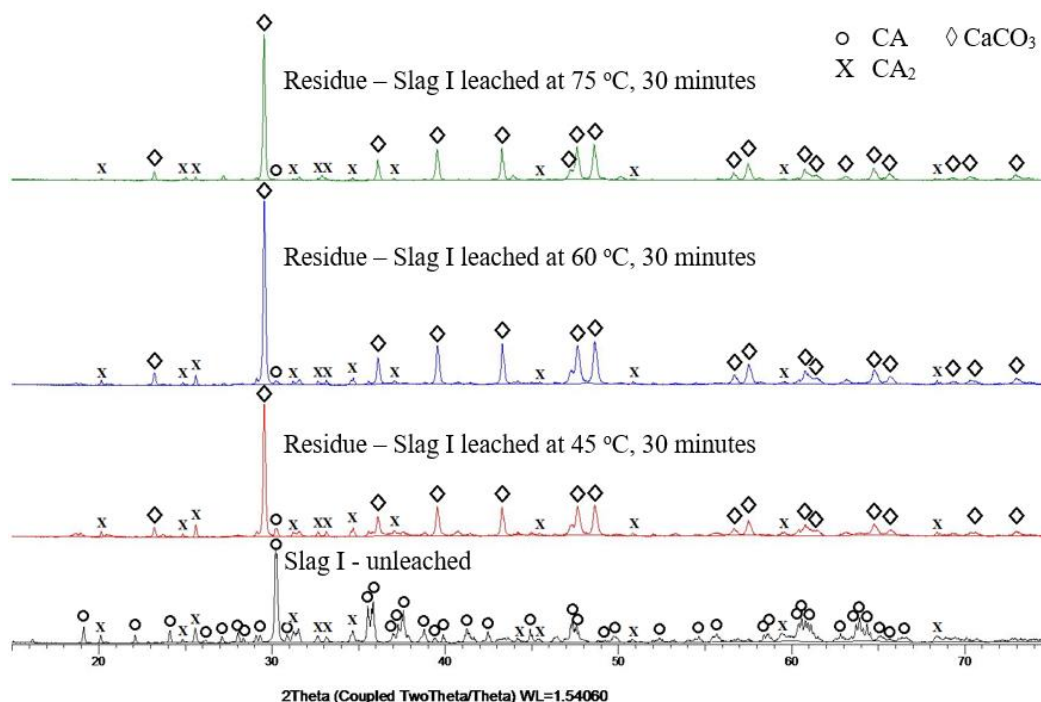
3.2. Characterization of Leach Residue

Figure 6. XRD pattern of Slag I residue after leaching at 45 ^{o}C, 60 ^{o}C, and 75 ^{o}C for 30 minutes.
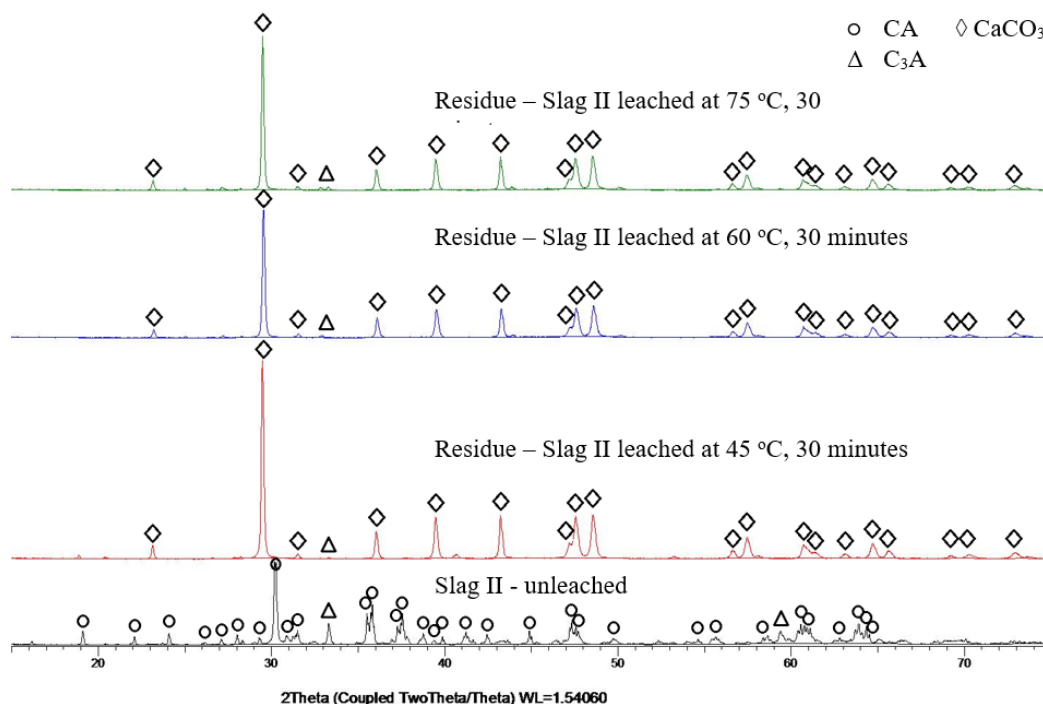

Figure 7. XRD pattern of Slag II residue after leaching at 45 ^{o}C, 60 ^{o}C, and 75 ^{o}C for 30 minutes.

After a series of leaches at different temperatures and times, the extent of CA, CA_2, and C_3A leaching was measured. Figures 6 and 7 show XRD patterns of leached Slag I and II at 45 ^{o}C,

60 °C, 75 °C after 30 minutes. It can be seen that the main phase of the residue is $CaCO_3$ and all three phases of calcium aluminate are leachable.

3.1. Effect of Temperature

The effect of temperature in digestion is significant as stated in previous studies [15 – 18]. In this work, slags are leached at relatively low temperature, i.e. 45 °C, 60 °C, and 75 °C, compared to the commercial Bayer process. Lower temperature means lower energy, which is favorable in regards to production cost in industry.

3.1.1. Leachability of CA Phase

The leaching extent of the calcium aluminate phase is calculated semi quantitatively by means of XRD analytical software then multiplied to the resulting mass of residue in the experiment. The calculation is described in Equation (4).

$$\eta_{leach} = \left(\frac{mass_{initial} - \left(wt.\%_{SQ} \times mass_{residue} \right)}{mass_{initial}} \right) \times 100\% \qquad (4)$$

where:
η_{leach}	Leachability of phase, %
$mass_{initial}$	Initial mass of phase, g
$wt.\%_{SQ}$	Semi quantitative weight fraction of phase, %
$mass_{residue}$	Mass of sample residue, g

The semi-quantitative leaching extent of the CA phase from Slag I and II can be seen in Figure 8. The leachability of CA in Slag I markedly increases from 79.2 %, 89.9 %, to 98.2 % by increasing the temperature from 45 °C, 60 °C, to 75 °C, respectively. While in Slag II, the leaching rate is quite stable at 94.5 % and 95.3 % at 45 °C and 60 °C respectively, increasing to 97 % at 75 °C. As observed here and mentioned in the literature [3, 20, 22, 23], CA is a soluble phase in sodium carbonate solutions. It is found here that CA_2 as the other phase present in Slag I hinders the leachability of CA. Further discussion on this observation, as well as CA_2 leachability is in section 3.1.2.

In principle, the leaching rate is associated with the reaction kinetics and their activation energies. The higher the activation energy of a reaction, the more sensitive the reaction to the temperature, and likely to be chemical rate controlling. It is worth noting that Abdel-Aal [15], Pereira et al. [16], and Yang et al. [17] showed that gibbsitic alumina digestion is chemical rate controlled. Until recently, Tong and Li [18] reported that calcium aluminate digestion is diffusion controlled, and temperature has less effect. It is obvious the different conclusions resulted from different composition and phases of alumina, experimental condition, etc. By using HSC 7.1 software, the change of enthalpy (ΔH) during digestion in different calcium aluminate phases can be calculated as shown in Figure 9.

The digestion of all three phases existing in the slags are through exothermic reactions. The order of energy release during reaction from the highest to the lowest is C_3A, CA_2, and CA. In other words, at a given leaching temperature, Slag I has two leachable phases that could accumulatively give more energy to the system than Slag II could have. However, since the CA_2 phase has low leachability, either advantageous or disadvantageous effects on the kinetic leaching rate is not clearly confirmed.
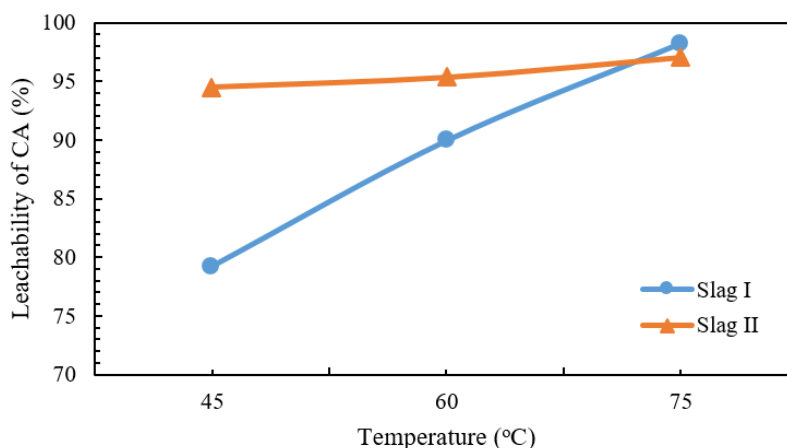
Figure 8. Leachability of CA phase on Slag I and Slag II at 45 ^{o}C, 60 ^{o}C, and 75 ^{o}C in 30 minutes.
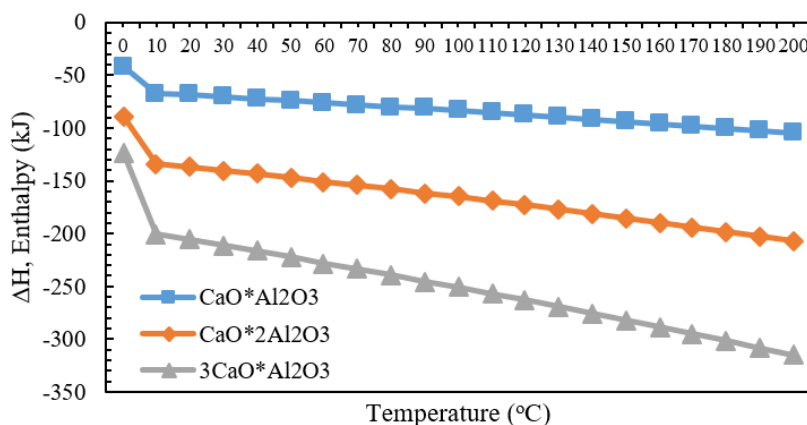

Figure 9. Change of enthalpy in digestion for different calcium aluminate phases.

3.1.2. Leachability of CA$_2$ Phase

As can be seen in Figure 10, the leachability of the CA$_2$ phase in Slag I after 30 minutes is 6.2 %, 15 %, and 69 % at 45 ^{o}C, 60 ^{o}C, and 75 ^{o}C , respectively. Below 45 ^{o}C, the CA$_2$ phase is practically insoluble. However, this leaching behavior is similar to that of the CA phase in Slag I (see Figure 8). Therefore, the hinder effect of CA$_2$ phase to CA leachability is apparent.

According to Equation (2), the leaching reaction of 1 mol of this phase needs 2 mol NaOH. In this work, the solvent concentration is fixed and sodium hydroxide concentration is relatively low; 2 times higher than the stoichiometry. However, this phase cannot be leached in a pure solution of sodium hydroxide due to CaO in the reduction slag reacting with NaOH to form Ca(OH)$_2$ which is followed by a reaction with NaAl(OH)$_4$ to form tricalcium hydro-aluminate (3CaO.Al$_2$O$_3$.6H$_2$O). This phenomenon gives lower yield to the alumina production, as reported by Wang et al. [19]. Therefore, it is of importance to ensure an adequate concentration of NaOH and Na$_2$CO$_3$ in the solvent to leach CA$_2.$
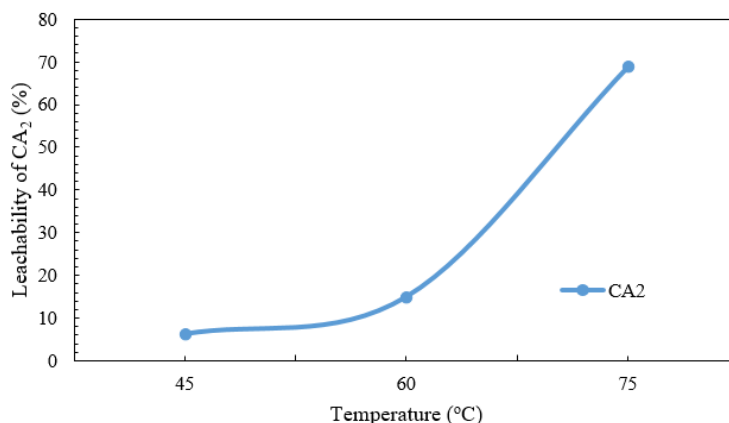
Figure 10. Leachability of CA$_2$ phase at 45 ^{o}C, 60 ^{o}C, and 75 ^{o}C after 30 minutes.

3.1.3. Leachability of C$_3$A Phase

It has been reported that the C$_3$A phase is difficult to leach and less than 50 % soluble in a 5 % solution of Na$_2$CO$_3$ [20, 21]. The present experimental results in Figure 11 show that the leachability of the C$_3$A phase at 45 ^{o}C, 60 ^{o}C, and 75 ^{o}C after 30 minutes of holding time are 46.7 %, 58.4 %, and 65 %, respectively. This indicates that the leachability of C$_3$A phase is higher than CA$_2$ at same given conditions.
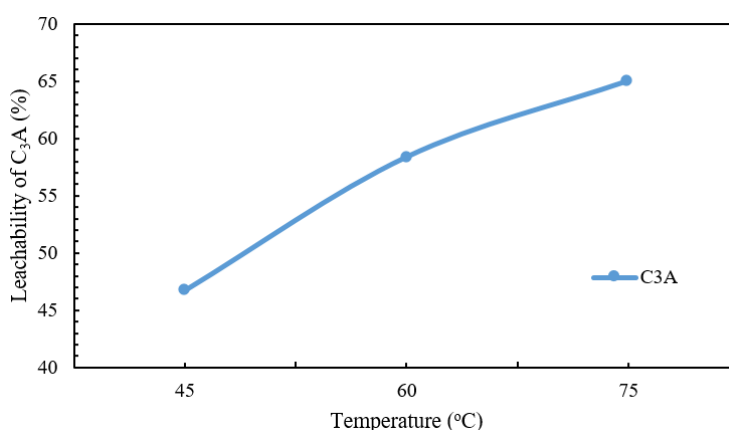

Figure 11. Leachability of C$_3$A phase in Slag II at 45 ^{o}C, 60 ^{o}C, and 75 ^{o}C after 30 minutes.

3.2. Effect of Leaching Duration

The leachability of CA and CA$_2$ phases in Slag I at different leaching times are shown in Figure 12. Consecutively, the CA leaching rate is 77.8 %, 79.2 %, and 95.4 % at 15, 30, and 60 minutes. While the CA$_2$ phase is leached to the extent of 0.2 %, 6.2 %, and 10.4 %.

It is worth noting that for the CA phase, leaching at 45 ^{o}C for 60 minutes could give a similar leaching rate as at 75 ^{o}C for 30 minutes. While for the CA$_2$ phase, the duration of leaching does not change dramatically the extent of leaching.
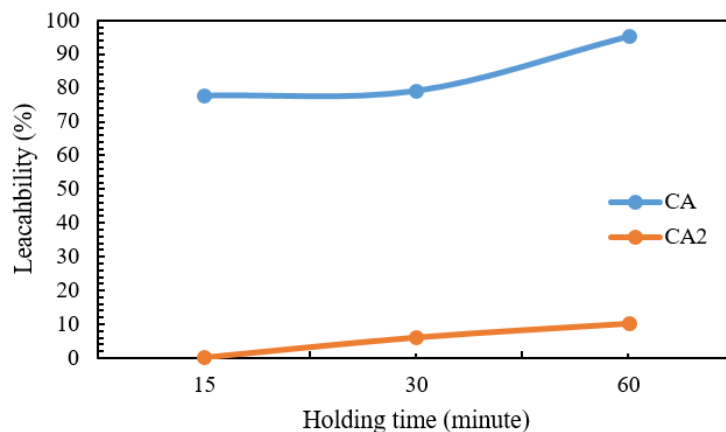
Figure 12. Extent of Leaching of CA and CA$_2$ phases in Slag I at 45 ^{o}C at different holding times.

4. Conclusions

Synthetic high purity calcium aluminate slags were prepared, pulverized, and subsequently leached by solutions containing Na$_2$CO$_3$ and NaOH at different temperatures and durations. The main results regarding the leachability of the slags can be summarized as:

1. Increased temperature significantly enhances the leachability. Moreover, the effect of temperature is dependent on the type and amount of phases in the slags.

2. The rate of leaching is fast and significant digestion occurs within relatively short reaction times. However, the extent of leaching in a given duration is dependent on the slag type.

3. In binary calcium aluminate slags, the leachability of one phase affects the leaching behavior of the other ones. The leachability of the CaO.Al$_2$O$_3$ phase in Slag I is hindered by the presence of the less leachable CaO.2Al$_2$O$_3$ phase.

4. The leachability of studied calcium aluminate phases in binary slags from highest to the lowest is CaO.Al$_2$O$_3$, 3CaO.Al$_2$O$_3$ and CaO.2Al$_2$O$_3$.

Acknowledgement

References

1. Peter Smith, The processing of high silica bauxites – review of existing and potential processes, *Hydrometallurgy*, 2009, 162-176.
2. M. Jiayu, L. Zhibao, and X. Qinggui, A new process for Al$_2$O$_3$ production from low-grade diasporic bauxite based on reactive silica dissolution and stabilization in NaOH-NaAl(OH)$_4$ media, *American Institute of Chemical Engineers*, 2012, Vol. 58, No. 7, 2180-2191.
3. H.E. Blake Jr. et al., Adaptation of the Pedersen process to the ferruginous bauxites of the pacific northwest, *US Bureau of Mines Report Investigations*, No. 6939, 1968, 1-24.

4.   Jafar Safarian and Leiv Kolbeinsen, Smelting-reduction of bauxite for sustainable alumina production, *Sustainable Industrial Processing Summit*, 2016, 1-8.

5.   H. Sellæg, L. Kolbeinsen, and J. Safarian, Iron separation from bauxite through smelting-reduction process, *Light Metals* 2017, 127-135.

6.   H. Pedersen, Process of manufacturing aluminum hydroxide, *US Patent Office*, No. 1618105, 1927.

7.   R.V. Lundquist and H. Leitch, Aluminium extraction characteristics of three calcium aluminates in water, sodium hydroxide, and sodium carbonate solutions, *US Bureau of Mines Report Investigations*, Nevada, 1964, 1-16.

8.   Z. Tong, Y. Li, L. Lian, Influence of titania on phase composition and self-powder and alumina leaching properties of calcium aluminate slag, *Light Metals* 2012, 185-188.

9.   Wang et al., Effect of calcium/aluminium ratio on MgO containing calcium aluminate slags, *Light Metals* 2011, 201-204.

10.   Wang et al., Synergistic effect of $C_{12}A_7$ and CA on alumina leaching property under low calcium/aluminum ratio, *Light Metals* 2015, 59-62.

11.   Wang et al., Effect of Na_2O on alumina leaching property and phase transformation of MgO-containing calcium aluminate slags, *Transactions of Nonferrous Metals Society of China*, 2011, 2752-2757.

12.   D.A. Jerebtsov and G.G. Mikhailov, Phase diagram of $CaO-Al_2O_3$ system, *Ceramics International*, 2001, 25-28.

13.   Bengt Hallstedt, Assessment of the $CaO-Al_2O_3$ system, *Journal of the American Ceramic Society*, 1990, 15-23.

14.   R.W. Nurse, J.H. Welch, and A.J. Majumdar, The $12CaO.7Al_2O_3$ phase in the CaO - Al_2O_3 system, *Transactions of the British Ceramic Society*, Vol. 64, 1965.

15.   E.S.A. Abdel-Aal, Leaching kinetics of gibbsitic bauxite with sodium hydroxide, *E3S Web of Conferences* 8, 2016.

16.   Pereira et al., The kinetics of gibbsite dissolution in NaOH, *Hydrometallurgy*, 2008.

17.   Yang et al., Dissolution kinetics and mechanism of gibbsitic bauxite and pure gibbsite in sodium hydroxide solution under atmospheric pressure, *Transactions of Nonferrous Metals Society of China*, 2015.

18.   Z. Tong and Y. Li, Leaching behavior of alumina from smelting reduction calcium aluminate slag with sodium carbonate solution, TMS, *Light Metals*, 2017.

19.   Wang et al., Study on extracting aluminum hydroxide from reduction slag of magnesium smelting by vacuum aluminothermic reduction, *Light Metals* 2011, 205-209.

20.   O.C. Fursman, H.E. Blake Jr., J.E. Mauser, Recovery of alumina and iron from pacific northwest bauxites by the Pedersen process, *US Bureau of Mines Report Investigations*, No. 7079, 1968, 1-22.

21.   Wang et al., The effect of cooling rate on the leachability of calcium aluminate slags, *Light Metals* 2011, 241-244.

22.   Jan Miller and Aake Irgens, Alumina production by the Pedersen process – history and future, *Light Metals* 1974, 977-982.

23.   Jafar Safarian and Leiv Kolbeinsen, Sustainability in alumina production from bauxite, *Sustainable Industrial Processing Summit*, 2016.